Pilz, M., Parolai, S., Picozzi, M., Zschau, J. (2011): Evaluation of proxies for seismic site conditions in large urban areas: the example of Santiago de Chile. - Physics and Chemistry of the Earth, 36, 16, 1259-1266

DOI: 10.1016/j.pce.2011.01.007

# Evaluation of proxies for seismic site conditions in large urban areas: the example of Santiago de Chile

Marco Pilz (a,b,*), Stefano Parolai (a), Matteo Picozzi (a), Jochen Zschau(a)

(a) Helmholtzzentrum Potsdam – German Research Center for Geosciences
Telegrafenberg
14473 Potsdam
Germany

(b) Universität Potsdam
Institut für Erd- und Umweltwissenschaften
Karl-Liebknecht-Str. 24
14476 Potsdam
Germany

(*)corresponding author
Helmholtzzentrum Potsdam – German Research Center for Geosciences
Telegrafenberg
14473 Potsdam
Germany
pilz@gfz-potsdam.de
Tel. +49 331 288 28664
Fax +49 331 288 1204

Abstract

Characterizing the local site response in large cities is an important step towards seismic hazard assessment. To this regard, single station seismic noise measurements were carried out at 146 sites in the northern part of Santiago de Chile. This extensive survey allowed the fundamental resonance frequency of the sedimentary cover, derived from horizontal-to-vertical (H/V) spectral ratios, to be mapped. By inverting the spectral ratios under the constraint of the thickness of the sedimentary cover, known from previous gravimetric measurements, local S-wave velocity profiles have been retrieved. After interpolation between the individual profiles, the resulting high resolution 3D S-wave velocity model allows the entire area, as well as deeper parts of the basin, to be represented in great detail. Since one lithology shows a great scatter in the velocity values only a very general correlation between S-wave velocity in the uppermost 30 m ($v_s^{30}$) and local geology is found. Local S-wave velocity profiles can serve as a key factor in seismic hazard assessment, since they allow an estimate of the amplification potential of the sedimentary cover. Mapping the intensity distribution of the 27 February 2010 Maule, Chile, event (Mw=8.8) the results indicate that local amplification of the ground motion might partially explain the damage distribution and encourage the use of the low cost seismic noise techniques for the study of seismic site effects.

Keywords: ambient seismic noise, H/V ratio, inversion, S-wave velocity, site effects

1. Introduction

Urbanization is one of the most dramatic processes of global change. The global proportion of urban population rose dramatically from 13% (220 million) in 1900 to 49% (3.2 billion) in 2005 and is likely to rise to 60% (4.9 billion) by 2030 (Population division of the UN 2005). Furthermore, the demographic explosion focuses more and more on large urban agglomerations with more than one million inhabitants. Nowadays, more than 38% of people worldwide live in cities with more than one million inhabitants. Many of the world's largest cities have developed in regions with wide plains of fluvial deposits or lakeshores and estuaries with water-saturated sediments, sites with seismically unfavorable properties. Given this spread of urban populations into areas of unfavourable soils all over the world, future earthquakes might cause extensive human and economic damage, since geometrical and mechanical features of alluvial deposits have great influence on seismic wave propagation and amplification as seen from many recent events. The Michoacan, Mexico, event (1985, Mw=8.1) and the Hyogo-ken Nanbu, Japan, earthquake (1995, Mw=6.9) can serve as notable examples of the consequences of such site effects.

Among the most destructive phenomena associated with plate tectonic motion is the occurrence of severe earthquakes. Remarkably, sixty percent of worldwide casualties associated with natural disasters are due to earthquakes (USGS 1998). Mitigation of the consequences of such events, including the loss of life, property damage, and social and economic disruption, depends on reliable seismic hazard estimates for land use planning, improved building design and construction (including adoption and enforcement of building construction codes), emergency response preparedness plans, and housing and employment decisions. To this regard, seismic microzonation studies are considered an important component of the assessment of seismic hazard in urban areas in terms of the assessment of

soil amplification, risks of liquefaction potential, and slope failure that might be caused during earthquakes.

In particular, local geological conditions can produce significant modifications in the ground motion during earthquakes. One way of estimating such local effects is by means of empirical methods that are based on the analysis and treatment of records (see Aki (1988) for an extensive review). In general, the experimental methods can be subdivided into reference site and non-reference site techniques (e.g. Bard 1995). The reference site technique, first proposed by Borcherdt (1970), consists of comparing records at nearby sites using one of them as the reference site. It is assumed that records at the reference site (usually a station installed on outcropping hard rock) contain the same source and propagation effects as records from other sites of the network. Therefore, differences that are observed between the sites are explained to be caused by local site effects. A major drawback of this method is that a suitable reference site may not always be available (Steidl et al. 1996). To this regard, non-reference site techniques such as the horizontal-to-vertical spectral ratio method, first introduced by Nogoshi and Igarashi (1970, 1971), have become popular for such areas.

Nakamura (1989) further developed this technique as a means of estimating the site response due to S-waves. Originally, the method was intended for interpreting measurements of ambient seismic noise (NHV) but Lermo and Chavez-Garcia (1993) applied the H/V technique to S-waves of earthquake recordings. In the last few years this approach has been applied by a great number of seismologists and engineers to characterize the seismic hazard on a local scale and of providing detailed information for seismic microzonation in urban areas (e.g. Fäh et al. 2001, Arai and Tokimatsu 2004). In particular, this technique stands out due to several advantages: only one seismic station with three components is needed, and it is not necessary to wait for the occurrence of an earthquake since microtremors provide the input motion. Parolai et al. (2001, 2004) showed that the NHV spectral ratios exhibit good agreement with the H/V from earthquake recordings, especially in terms of the value of the

fundamental resonance frequency of the sedimentary cover. However, higher harmonics are often not visible in the H/V spectra, but may not necessarily be damped out, and the method allows only a lower bound estimate of the amplification.

Further support for microzonation studies might therefore be based on modeling of realistic ground motion scenarios. This requires a further characterization of local site conditions especially in terms of local shear-wave velocity profiles. Aki (1957) used small-scale seismic arrays and derived the phase velocity dispersion curve by correlating the noise recordings. Later studies (e.g. Horike 1985) aimed at improving the results from such array measurements. Often, information is obtained through active in-situ measurements and invasive techniques such as drilling, down/cross-hole measurements, etc. (e.g. Tokimatsu et al. 1991, Fäh et al. 2001, Arai and Tokimatsu 2004). However, especially in urban areas, making use of explosive sources is almost impossible, and the expensive nature of invasive methods requires a compromise between a widespread application of such techniques and a limited exploration depth. Partly due to the limited exploration depth of invasive methods, microzonation studies are frequently based on the use of the average shear wave velocity in the uppermost 30 m ($v_s^{30}$) which is adopted by the National Earthquake Hazard Reduction Program (NEHRP) classification in the USA (Building Seismic Safety Council 2004). The original work of Borcherdt (1992) was based on data from the western USA, and so were the first papers discussing advantages (Anderson et al. 1996) and disadvantages (Wald and Mori 2000) of the method. Outside the region where the method was developed, some doubts arose about the capability of $v_s^{30}$ to predict amplification in deep basins (Park and Hashash 2004) and in other tectonically active regions (Stewart et al. 2003). Nevertheless, $v_s^{30}$ serves as a default parameter for many building codes worldwide which, in turn, yields to the need to find proxies for it. A new approach that the slope of topography might allow a first-order site classification (Wald and Allen 2007, Allen and Wald 2009) might be useful for regional studies but is not intended for microzonation of urban areas (Pilz et al. 2010). With $v_s^{30}$ being

the parameter mostly used, several publications (Scherbaum et al. 2003, Ohrnberger et al. 2004, Parolai et al. 2006, Castellaro and Mulargia 2009) showed that reliable values of the S-wave velocity can be obtained by an inversion of H/V curves once the total thickness of the sedimentary cover is constrained. Moreover, measurements of ambient seismic noise are easy to perform and feasible even in densely populated areas. So, combined with shallow geophysical investigations, this technique is therefore suitable as a simple and fast technique for an evaluation of seismic site conditions, especially in large urban areas.

The exposure of the city of Santiago de Chile, the country´s capital with more than six million inhabitants, to a significant seismic hazard allows checking the method. The main factor controlling the hazard for Santiago de Chile is the ongoing subduction of the Nacza plate under the South American plate along the Peru-Chile trench. Return periods of magnitude 8 events are on the order of around 12 years for the entire country (Barrientos et al. 2004). Furthermore, the city is located in a narrow basin between the Andes and the coastal mountains filled with soft sediments that may strongly modify seismic motion. This was realized during the 1958 Las Melosas sequence (Mw=6.7-6.9) and the 1985 Valparaiso (Mw=8.0) event (e.g. Çelebi 1987, Sepulveda et al. 2008) and also recently during the 2010 Chile (Mw=8.8) earthquake. In particular, some parts of the city suffered significant damage, largely due to amplification of earthquake ground motion. The anomalous amplification of ground motion observed in these parts of the city is considered mainly to be related to the presence of soft sediments overlaying the competent igneous bedrock. The thickness and the S-wave velocity of the sedimentary layers as well the impedance contrast between the sediments and the underlying bedrock are the main local parameters affecting the frequency band and the peak values of seismic motion that may be strongly amplified by the local conditions. It is therefore of utmost importance to check if any correlation between the parameters of $v_s^{30}$, surface geology, and intensity may exist. Several investigations have been conducted in Santiago de Chile to evaluate site effects in the city (Midorikawa et al. 1991,

Cruz et al. 1993, Toshinawa et al. 1996, Bonnefoy-Claudet et al. 2009, Pilz et al. 2009, 2010). Moreover, data of the 2010 Maule event will also allow a first comparison with previous results.

In our study we focus on the question of wither the profile of the S-wave velocity, which can be determined by measurements of the seismic noise, can provide a reliable estimation of site effects. We first give a short overview of the geological conditions and the setup used for the experiments. Second, we will give some information about the S-wave velocity model of the Santiago basin. Finally, we qualitatively compare these results with intensity values determined after the 2010 Maule earthquake.

## 2. Geological setting

The city of Santiago de Chile is located in the so-called Central Depression, which is a basin surrounded by the Main and Coastal ranges of the Andes. This large bowl-shaped basin spans for 80 km by 30 km wide, mainly elongated in the north-south direction. Volcanic activity dated between the upper Oligocene and lower Miocene is believed to have formed the basement of the Santiago basin. Its bottom, only indirectly known from gravimetric measurements (Araneda et al. 2000), corresponds to an uneven surface unveiled by some buried hill chains that locally outcrop within the basin (e.g. Cerro Renca, Cerro San Cristóbal,).

The basin itself is essentially filled with alluvial sediments, most of which have been transported from the Andes mountains by a complex river system (Valenzuela 1978). Due to the uneven bedrock shape, the thickness of the sedimentary cover varies over short distances

and can exceed more than 550 m in the western part of the city (Lo Prado and Pudahuel districts).

The sediments themselves are mainly composed of gravel, sand, clay and volcanic ashes. Clayey material is most common in the north whereas the gravels are in the eastern and southern part of the basin near the apexes of alluvial fans. Volcanic ash (pumice) accompanied by fragments of rocks are also observed at the surface of the basin (Pudahuel district) probably resulting from a major eruption of the Maipo volcano, located 120 km to the south-east, 450 000 years ago (Baize et al. 2006). The thickness of volcaniclastic material, with interlayered sand and gravel, can reach more than 40 m in some areas.

A simplified map of the surface geology is shown in Figure 2; for further details see Leyton et al. (2010) and Valenzuela (1978). Composition and thickness of subsurface layers remains uncertain due to sharp lateral and vertical variations of some geological units. One must therefore keep in mind that the basin geometry is far more complex than has been mapped here.

## 3. Data acquisition

The first experiment was carried out from 19 May until 13 June 2008 and aimed at recording ambient seismic noise by using single station seismic noise measurements. Data were recorded at 146 sites (Figure 3) using an EarthData logger PR6-24 instrument connected to a Mark L-4C-3D sensor with GPS timing. We used sensors with a resonance frequency of 1 Hz and a maximum possible gain (i.e. 10) for the digitizer with which allows detection of H/V peaks down to 0.1 to 0.2 Hz (Strollo et al. 2008a, Strollo et al. 2008b). At each site, the signal was recorded for at least 25 minutes with a sampling rate of 100 samples per second for the

statistical stabilization of the signal. For almost all the measurements, the sensor was placed directly on the ground (i. e. mown grass, not overgrown soil), with only a few measurements carried out on asphalt. On some days rain had been slight to moderate, but it has been shown (Chatelain et al. 2008) that no noticeable influence is expected to be caused by rain. For all measurements, the sensor was protected against wind, and no measurements were made in the immediate vicinity of trees or buildings.

## 4. Data analysis

Due to their inexpensiveness, many studies focused their attention on the analysis of NHV measurements and agreed that the H/V spectral ratio of seismic noise provides a fair estimate of the fundamental resonance frequency of a site where there is a large impedance contrast between the sediments and the bedrock (Lermo and Chavez-Garcia 1994, Field and Jacob 1995, Horike et al. 2001, Bard 2004). Where the fundamental frequency (or higher modes) of the soil overlaps with the frequencies of man-made structures amplification effects may strongly increase the structural response, which may lead to increased damages of the structures. For this purpose, the recorded microtremor signals were systematically analyzed for each measurement site considering the recommendations proposed by the SESAME consortium (Bard and SESAME WP02 team 2005).

By interpolating between the individual measurement sites the fundamental resonance frequency of the soil was mapped for the investigated area (Figure 3). Almost the entire area is characterized by frequencies well below 2 Hz. Only when one considers sites close to the city centre and around the Cerro San Cristóbal, the fundamental frequency does increase more rapidly. In this part of the basin, the thickness of the sedimentary cover is decreasing rapidly

and the bedrock outcrops. As outlined in Pilz et al. (2009), clear NHV peaks, i.e. a large impedance contrast between the unconsolidated sediments and the bedrock, are located in the northern and western part of the investigated area. Flat NHV curves and peaks with low amplitude are predominantly in the eastern areas where the surface consists of dense sediments, in agreement with Bonnefoy-Claudet et al. (2009).

Recently, the possibility of retrieving the S-wave velocity structure below a site from single station measurements based on NHV ratio computation was tested by Fäh et al. (2001). After having shown that there is a good agreement between the NHV ratio and the theoretical ellipticity curves of the fundamental mode Rayleigh wave they proposed to invert the NHV curve to directly obtain the S-wave velocity profile. Due to the nonlinear nature of the problem, the inversion procedure is based on a genetic algorithm (Fäh et al. 2001, 2003) and is carried out for a fixed number of layers (generally seven; only four, if the thickness of the sedimentary cover is below 50 m) and the assumption of a one-dimensional structure below the site using wide ranges of geophysical properties. Since an infinite number of structural models leading to the same H/V spectrum exist, additional information is needed to constrain the inversion.

For the Santiago basin, we applied the technique proposed by Fäh et al. (2001, 2003) with the constraint of the total thickness of the sediments, which is known from gravimetric measurements (Arandea et al. 2000). That condition allows avoidance of trade-off between total thickness and the S-wave velocity profile. There is, however, some degree of uncertainty in the topography of the bedrock due to the interpolation of the gravimetric data between the measurement sites, since the sites were spaced with an interstation distance of around 500 m. Therefore, the total thickness of the sediments was allowed to vary within 10 % compared to the estimated value derived by the gravimetric data to account for uncertainties.

In the end, the model that, amongst all those generated, allows the best reproduction of the observed NHV, is chosen as the best model. By interpolation between the individual S-wave

velocity profiles a 3D velocity model of the investigated area was derived. Pilz et al. (2010) tested the validity of the interpolated model by comparing with available geological data sets from literature and described that the model is able to reliably point out local characteristics of other data sets, but takes advantage of the fact that all individual S-wave velocity profiles reach the bedrock. Cross-sections of the S-wave velocity model are shown in Figure 4. As expected, all profiles show a trend of increasing S-wave velocities with depth, but strong lateral velocity differences, even within the single units, caused by lateral and vertical variations of the physical properties, are found. To the east of Cerro San Cristóbal, the S-wave velocity and the velocity gradient are higher than to the west (Figure 4.1). As already mentioned, flat H/V curves and H/V spectral ratios of low amplitude are mainly located in the eastern parts of the basin over dense sediments, i.e. gravel. These parts of the basin are characterized by the high seismic velocities of the sediments leading to small velocity contrasts with the bedrock. On the contrary, superficial fine-grained material, found in the western parts of the investigated area and characterized by low shear wave velocities, can clearly be identified (Figure 4.2). To the south-west of the investigated area (Pudahuel and Lo Prado districts, see Figure 1), the thick layer of pyroclastic flow deposits, outcropping at the top of the filling and showing a shear wave velocity well below the velocity of the surrounding materials, is considerably visible (Figure 4.3).

## 5. Comparison of S-wave velocity, site response, and macroseismic intensity for the 2010 Maule earthquake

On 27 February 2010 an Mw=8.8 earthquake occurred offshore the Maule region, Chile. The epicenter was located 335 km south-west of Santiago de Chile but the rupture continued

almost until the latitude of Santiago. In particular, the level of macroseismic intensity was found to be remarkably different within the city. In general, many modern houses and other structures were largely unaffected due to high anti-seismic building codes but a large number of structures were heavily damaged, including three hospitals and many government buildings and ministry headquarters.

To investigate building damage and seismic intensities, we followed the European Macroseismic Scale (EMS98). EMS98 is a macroseismic scale proposed by the European Seismological Commission of International Association of Seismology and Physics of Earth's Interior (IASPEI), which was modified from the MSK scale to be applicable to various modern structures.

To compare macroseismic intensity with $v_s^{30}$ values, we choose to characterize the relationship in terms of discrete steps in S-wave velocity according to the U.S. National Earthquake Hazards Reduction Program (NEHRP) $v_s^{30}$ boundaries (Building Seismic Safety Council 2004). Moreover, to increase resolution, the NEHRP boundaries are further subdivided into narrower velocity ranges, following Wald and Allen (2007). We mapped $v_s^{30}$ for an area limited by a linear connection between the outermost measurement sites (Figure 5). In consistency with the cross-sections shown in Figure 4 different S-wave velocities in the uppermost 30 m can clearly be identified. When comparing our $v_s^{30}$ map with the intensity values determined for the earthquake there seems to be a tendency that the intensity distribution for that event is at least partially influenced by local variations of $v_s$.

Most of the damages are observed in municipalities located in the western and north-western part of the city (Pudahuel, Renca, Cerro Navia, Lo Prado municipalities, see Figure 1) where a small-sized low-quality building stock can be found (Astroza et al. 1993). Although most of the houses in this area seem to be old and characterized by a high vulnerability the properties of the soil are different to the ones in the rest of the city, and this affected the level of intensity. A few adobe houses were completely destroyed, many adobe and simple masonry

buildings suffered significant damage (Figure 6 a). Also few masonry buildings with steel frame show moderate to substantial damage, an expected behavior (Moroni et al. 2004). Two overpasses on the highway fully and another two showing minor structural damage. Altogether, this indicates the EMS intensity to be VIII. Yet a comparison of NHV peak frequencies and damage on small-size houses reveals a discrepancy; although the NHV peak frequencies do not exceed 1-2 Hz, much damage was observed especially on houses, for which the natural frequency is expected to be much higher. Lowest $v_s^{30}$ values are found in that area, with the smallest $v_s^{30}$ values for the pumacit layer, situated on the top of sedimentary filling and clearly visible as a red ellipse in Figure 5.

In the business district in the central northern part (south-eastern part of Huechuraba, see Figure 1) many (in general modern reinforced concrete) buildings have been partially and seven of them totally destroyed (Bray and Frost (2010), Figure 6 b). Considering that, although these structures are new (less than ten years) and should have been constructed according to recent building codes, most of them have five to ten floors. Since the fundamental resonance frequency of the soil in this area is around 0.7 to 1 Hz (Figure 3) the high damage might be due to an overlap of the resonance frequencies of the soil and the present structures, following Guendelmann (2000). Moreover, also the central part of Huechuraba several masonry buildings suffered significant damage (e.g. collapsed municipality building). Since highest NHV amplitude values are found in that area, this suggests that ground motion might have been relatively strong. We estimate an intensity of VII to VIII for that area.

In the central and eastern parts (municipalities of Santiago, Providencia) the building stock generally consists of modern buildings with steel and reinforced concrete frame as well as steel frame buildings; no adobe houses are present (Figure 6 c). Most of these buildings performed well with no or minor damage to finishes and non-structural features. This suggests that the intensity might be one to two degrees below the values found for the western parts.

This area also shows lower H/V peak amplitudes and generally higher $v_s^{30}$ values. Since the fundamental resonance frequency of the soil is higher in this area no overlap with the resonance frequency of the buildings is expected. We estimate the intensity to be VI to VII.

In the far eastern districts (Las Condes and surrounding municipalities) buildings are generally modern residential structures up to four floors. No damage is observed in these buildings. NHV peak amplitudes and $v_s^{30}$ values are low. Five 17-story apartment blocks in the south-eastern part of Las Condes (Figure 6 d) are an exception. These buildings show structural damage, and two towers have been tilted (Daniel Hernández, personal communication). The reason for this behavior is not surprising since we determined the fundamental resonance frequency of the building by measurements on the top of one tower to be around 0.7 Hz (Figure 7). This frequency exactly coincides with the fundamental resonance frequency of the soil for a measurement site close-by. Moreover, also higher harmonics of the building can easily be seen in the spectra. It seems reasonable to assume that resonance effects are responsible for the damage distribution in that area.

Of course, only a general trend can be identified when mapping the fundamental frequency of the soil, NHV peak amplitudes, and $v_s^{30}$ values. No direct but only a slight correlation between NHV amplitude and damage is found. In particular, measurements carried out on Cerro San Cristóbal, showing high fundamental frequencies and high H/V peak amplitudes, do not follow this trend. One should therefore be aware of drawing any strict borders between individual units due to varying properties within the same range, indicating the incompleteness of each of the parameters to fully describe site effects.

At the moment, a combination of all mentioned parameters might allow the best, although still only very approximate, characterization of site conditions but, of course, no general conclusions should be drawn. $v_s^{30}$ is not the only factor controlling ground-motion amplification since further 3D effects caused by deep sedimentary basins and the surface topography might also modify the observed level of ground shaking.

To this regard, it is interesting to note that the high level of macroseismic intensity in the north-western parts of the studied area might also be enhanced by the trapping of seismic energy in the deepest parts of the basin. It seems also noteworthy that highest intensities are found especially around Cerro Renca and to the west and to the south of Cerro San Cristóbal (see Figure 5). Since the seismic waves of the 2010 Maule main shock entered the basin from south-western direction, the pronounced topography will have caused the waves to be largely reflected and scattered by the outcropping bedrock, leading to a strong increase in duration and level of shaking. Altogether, this serves as a further hint that not only near-surface conditions but several other parameters play a major role for ground motion complexity.

## 6. Conclusions

Local S-wave velocity profiles were derived for the northern part of the Santiago de Chile basin. Calculated NHV spectral ratios were systematically inverted under the assumption of a horizontally layered one-dimensional structure using information of the thickness of the sedimentary cover which has been determined previously by gravimetric measurements. By interpolating between individual S-wave velocity profiles a 3D model for the entire study area could be calculated showing large horizontal and vertical variations. When comparing $v_s^{30}$ values with the observed intensities following the 2010 Maule event, only a general trend can be identified showing higher intensities in areas with low $v_s^{30}$ values. However, in addition to near-surface site conditions seismic waves are also known to be influenced by sediment thickness and basin structure.

Although it remains impossible at the moment to reliably predict the occurrence and the impact of such events, this technique might help in identifying sites where strong shaking is

more likely to occur. Considering the relative low cost of this technique, a modest investment would allow, especially for cities located in areas prone to seismic risk, to contribute to seismic hazard assessment for the mitigation of urban earthquake risk and to desirable benefits in terms of human and economic losses avoided in the future.

Acknowledgements

This work was supported by the Helmholtz research initiative “Risk Habitat Megacity”. We are grateful David Solans, Natalia Silva, and José Gonzalez for assistance during the field work. Instruments were provided by the Geophysical Instrumental Pool Potsdam. We are also grateful to Lars Abrahamczyk for discussion about intensity distribution.

References


Aki, K. (1957): Space and time spectra of stationary stochastic waves, with special reference to microtremors, *Bull. Earthquake Res. Inst.* **35**, 415-456

Aki, K. (1988): Local site effect on ground motion, in *Earthquake Engineering and Soil Dynamics. II: Recent Advances in Ground-Motion Evaluation*, J. L. von Thun (ed.), *Am. Soc. Civil Eng. Geotechnical Spec. Publ.* **20**

Allen, T. I., D. J. Wald (2009): On the use of high-resolution topographic data as a proxy for seismic site conditions ($v_s^{30}$), *Bull. Seism. Soc. Am.* **99**, 935-943

Anderson J. G., Y. Lee, Y. Zeng, S. Day (1996): Control of strong motion by the upper 30 meters, *Bull. Seism. Soc. Am.* **86**, 1749-1759

Arai, H., K. Tokimatsu (2004): S-wave velocity profiling by inversion of microtremor H/V spectrum, *Bull. Seism. Soc. Am.* **94**, 53-63

Araneda, M., F. Avendano, C. Merlo (2000): Gravity model of the basin in Santiago, Stage III, *9th Chilenian Geological Congress* **2**, Santiago, Chile, 404-408

Astroza M., M. Moroni, M. Kupfer (1993): Calificación sísmica de edificios de albañilería de ladrillo confinada con elementos de hormigón armado, *Memorias de las XXVI Jornadas Sudamericanas de Ingeniería Estructural* **1**, Montevideo, Uruguay

Baize, S., S. Rebolledo, J. Lagos, R. Rauld (2006): A first-order geological model of the Santiago basin, *Conf. on 1906 Valparaíso Earthquake Centennial*, Valparaiso, Chile Paper NGT1-05

Bard, P. Y. (1995): Seismic input motion for large structures, *18th European Regional Earthquake Engineering Seminar,* Publication AFPS /EAEE, Vol. II

Bard, P. Y.: The SESAME project (2004): An overview and main results, *Proceedings of the 13th World Conference on Earthquake Engineering*, Vancouver, Paper 2207

Bard, P. Y., SESAME WP02 team (2005): Guidelines for the implementation of the H/V spectral ratio technique on ambient vibrations – measurements, processing and interpretations, *European Comission – Research General Directorate Project No. EVG1-CT-2000-00026 SESAME*, **D23.12**

Barrientos, S., E. Vera, P. Alvarado, T. Monfret (2004): Crustal seismicity in central Chile, *Journal of South American Earth Sciences* **16**, 759-768

Bonnefoy-Claudet, S., S. Baize, L. F. Bonilla, C. Berge-Thierry, C. R. Pasten, J. Campos, P. Volant, R. Verdugo (2009): Site effect evaluation in the basin of Santiago de Chile using ambient noise measurements, *Geophys. J. Int.* **176**, 925-937

Borcherdt, R. D. (1970): Effects of local geology on ground motion near San Francisco Bay, *Bull. Seism. Soc. Am.* **60**, 29-61

Borcherdt R. D. (1992): Simplified site classes and empirical amplification factors for site-dependent code provisions, *Proceedings of the NCEER, SEAOC, BSSC Workshop on Site Response during Earthquakes and Seismic Code Provisions*, Los Angeles, USA

Bray, J., D. Frost (2010): Geo-engineering reconnaissance of the February 27, 2010, Maule, Chile, earthquake, published online under http://www.geerassociation.org/ GEER_Post%20EQ%20Reports/Maule_Chile_2010/Cover_Chile_2010.html, last accessed 29 October 2010

Building Seismic Safety Council (BSSC) (2004): NEHRP recommended provisions for seismic regulations for new buildings and other structures, 2003 edition (FEMA 450), Building Seismic Safety Council, National Institute of Building Sciences, Washington, D. C., USA

Castellaro, S., F. Mulargia (2009): Vs30 estimates using constrained H/V measurements, *Bull. Seism. Soc. Am.* **99**, 761-773

Çelebi, M. (1987): Topographical and geological amplifications determined from strong-motion and aftershock records of the 3 March 1985 Chile earthquake, *Bull. Seism. Soc. Am.* **77** (4), 1147-1167

Chatelain, J. L., B. Guillier, F. Cara, A. M. Duval, K. Atakan, P. Y. Bard, SESAME WP02 team (2008): Evaluation of the influence of experimental conditions on H/V results from ambient noise recordings, *Bull. Earthq. Eng.* **6**, 33-74

Cruz, E., R. Riddell, S. Midorikawa (1993): A study of site amplification effects on ground motions in Santiago, Chile, *Tectonophysics* **218**, 273-280

Fäh, D., F. Kind, D. Giardini (2001): A theoretical investigation of average H/V ratios, *Geophys. Journ. Int.* **145**, 535-549

Fäh, D., F. Kind, D. Giardini (2003): Inversion of local S-wave velocity structures from average H/V ratios, and their use for the estimation of site-effects, *J Seism.* **7**, 449-467

Field, E. H., K. H. Jacob (1995): A comparison and test of various site-response estimation techniques, including three that are not reference-site dependent, *Bull. Seism. Soc. Am.* **85**, 1127-1143

Guendelman, T. (2000): Perfil bio-sismico de edificios. Un instrumento de calificacion sismica, *Revista BIT* **7**, 30-33

Horike, M. (1985): Inversion of phase velocity of long-period microtremors to the S-wave-velocity structure down to the basement in urbanized areas, *J. Phys. Earth.* **33**, 59-96

Horike, M., B. Zhao, H. Kawase (2001): Comparison of site response characteristics inferred from microtremor and earthquake shear waves, *Bull. Seism. Soc. Am.* **91**, 1526-1536

Lermo, J., F. J. Chavez-Garcia (1993): Site effect evaluation using spectral ratios with only one station, *Bull. Seism. Soc. Am.* **83**, 1574-1594

Lermo, J., F. J. Chavez-Garcia (1994): Are microtremors useful in site response evaluation? *Bull. Seism. Soc. Am.* **84**, 1350-1364

Leyton F., S. A. Sepúlveda, M. Astroza, S. Rebolledo, L. González, S. Ruiz, C. Foncea, M. Herrera, J. Lavado (2010): Zonificacion sismica de la Cuenca de Santiago, Chile, *Congreso Chileno de sismología e ingeniería antisísmica*, Valdivia, Chile

Midorikawa, S., R. Riddell, E. Cruz (1991): Strong-ground accelerograph array in Santiago, Chile, and preliminary evaluation of site effects, *Earthq. Eng. Struct. Dyn.* **20**, 403–407

Moroni, M.O., M. Astroza, C. Acevedo (2004): Performance and seismic vulnerability of masonry housing types used in Chile, *Journal of Performance of Constructed Facilities* **18**, 173-179

Nakamura, Y. (1989): A method for dynamic characteristics estimation of subsurface using microtremor on the ground surface, *Quaterly Reports of the Railway Technical Research Institute* **30**, 25-33

Nogoshi, M., T. Igarashi (1970): On the propagation characteristics estimations of subsurface using microtremors on the ground surface, *J. Seismol. Soc. Japan* **23**, 264-280

Nogoshi, M., T. Igarashi (1971): On the amplitude characteristics of microtremor, *J. Seismol. Soc. Japan* **24**, 26-40

Ohrnberger, M., F. Scherbaum, F. Krüger, R. Pelzing, S. K. Reamer (2004): How good are shear wave velocity models obtained from inversion of ambient vibrations in the Lower Rhine Embayment (N.W. Germany)?, *Bollettino di Geofisica teorica ed applicata* **45**, 215-232

Park, D., Y. Hashash (2004): Probabilistic seismic hazard analysis with non linear site effects in the Mississippi embayment, *13th World Conference on Earthquake Engineering*, Vancouver, Paper 1549

Parolai, S., P. Bormann, C. Milkereit (2001): Assessment of the natural frequency of sedimentary cover in the Cologne area (Germany) using noise measurements, *J. Earthq. Eng.* **5**, 541-564

Parolai, S., D. Bindi, M. Baumbach, H. Grosser, C. Milkereit, S. Karakisa, S. Zünbül (2004): Comparison of different site response estimation techniques using aftershocks of the 1999 Izmit earthquake, *Bull. Seism. Soc. Am.* **94**, 1096-1108

Parolai, S., S. Richwalski, C. Milkereit, D. Fäh (2006): S-wave velocity profiles for earthquake engineering purposes for the Cologne area (Germany), *Bull. Earthq. Eng.* **4**, 65-94

Pilz, M., S. Parolai, F. Leyton, J. Campos, J. Zschau (2009): A comparison of site response techniques using earthquake data and ambient seismic noise analysis in the large urban area of Santiago de Chile, *Geophys. J. Int.* **178**, 713-728

Pilz, M., S. Parolai, M. Picozzi, R. Wang, F. Leyton, J. Campos, J. Zschau (2010): Shear wave velocity model of the Santiago de Chile basin derived from ambient noise measurements: A comparison of proxies for seismic site conditions and amplification, *Geophys. J. Int.* **182**, 355-367

Population Division of the Department of Economic and Social Affairs of the United Nations Secretariat (2005): World Urbanization Prospects: The 2005 Revision, Pop. Division, Department of Economic and Social Affairs, New York, USA

Scherbaum, F., K. G. Hinzen, M. Ohrnberger (2003): Determination of shallow shear wave velocity profiles in the Cologne Germany area using ambient vibrations, *Geophys. J. Int.* **152**, 597-612

Sepulveda, S. A., M. Astroza, E. Kausel, J. Campos, E. A. Casas, S. Rebolledo, R. Verdugo (2008): New findings on the 1958 Las Melosas earthquake sequence, central Chile: Implications for seismic hazard related to shallow crustal earthquakes in subduction zones, *J. Earthq. Eng.* **12**, 432-455

Steidl, J. H., A. G. Tumarkin, R. J. Archuleta (1996): What is a reference site?, *Bull. Seism. Soc. Am.* **86**, 1733-1748

Stewart J. P., A. H Liu, Y. Choi (2003): Amplification factors for spectral acceleration in tectonically active regions, *Bull. Seism. Soc. Am*. **93**, 332-352

Strollo, A., S. Parolai, K. H. Jäckel, S. Marzorati, D. Bindi (2008a): Suitability of short-period sensors for retreiving reliable H/V peaks for frequencies less than 1 Hz, *Bull. Seism. Soc. Am.* **98**, 671-681

Strollo, A., D. Bindi, S. Parolai, K. H. Jäckel (2008b): On the suitability of 1 s geophone for ambient noise measurements in the 0.1 – 20 Hz frequency range: experimental outcomes, *Bull. Earthq. Eng.* **6**, 141-147

Tokimatsu, K., S. Kuwayama, S. Tamura, Y. Miyadera (1991): Vs determination from steady state Rayleigh wave method, *Soils and Foundations* **31**, 153–163

Toshinawa, T., M. Matsuoka, Y. Yamazaki (1996): Ground-motion characteristics in Santiago, Chile, obtained by microtremor observations, *11th World Conference on Earthquake Engineering*, Paris, Paper 1764

United States Geological Survey USGS (1998): Map of western hemisphere indicates location of potential earthquake damage, Reston, USA

Valenzuela, G. B. (1978): Suelo de fundación del Gran Santiago, *Inst. Invest. Geol. Santiago*, Santiago, Chile, Bol. **33**

Wald, L. A., J. Mori (2000): Evaluation of methods for estimating linear site-response amplifications in the Los Angeles region, *Bull. Seism. Soc. Am* **90**, 32-42

Wald, D. J., T. I. Allen (2007): Topographic slope as a proxy for seismic site conditions and amplification, *Bull. Seism. Soc. Am.* **97**, 1379-1395

Figure captions

Figure 1: Basin of Santiago de Chile. Locations mentioned in the text are indicated. The study area is marked by a black rectangle. Lines and numbers mark cross-sections shown in Figure 4. Letters indicate sites where pictures shown in Figure 6 have been taken. Borders between communities are marked in gray.

Figure 2: Simplified map of surface geology of the investigated area based on Valenzuela (1978) and Leyton et al. (2010).

Figure 3: Map of the fundamental resonance frequency of the investigated area. Black circles indicate microtremor measurement sites that have been considered for interpolation. White circles indicate sites where measurements have been carried out but no reliable value of the fundamental resonance frequency could be determined. Diameter of the spots corresponds to H/V peak amplitude. In the hatched area, no measurements were carried out; hence results are only due to interpolation.

Figure 4: Cross-sections of the interpolated 3D S-wave velocity model within the area of investigation. Locations of the profiles are indicated in Figure 1. Black triangles mark measurement sites within a distance of 500 m to the cross-section. (1) Lat 33.405° S, (2) Lon 70.730° W, (3) Lat 33.440° S, (4) Lon 70.635° W. For all profiles, topography is exaggerated about 16 times. The shape of the bedrock, shown in grey pattern, is derived from gravimetric data.

Figure 5: $v_s^{30}$ (NEHRP classification) for the area limited by a linear connection between the outermost measurement sites. In the shaded area, no measurements were carried out. Therefore, the results are only due to interpolation and are not plausible as outcropping bedrock can be found there. Roman numbers indicate estimated EMS intensity values. Areas of same intensity values are bordered by dashed lines.

Figure 6: Examples of different building stock and damage grade in the city of Santiago de Chile. Exact locations of the sites are indicated in Figure 1. a) Renca, adobe building. In traditional adobe construction, the four walls are often not joined together, making them especially unstable during earthquakes. b) Business district of Huechuraba, reinforced concrete structure. c) Modern building stock in the municipality of Providencia. d) Las Condes, damaged high rise structures surrounded by undamaged small building stock. See text for further discussion.

Figure 7: Top: H/V spectral ratio measured on the top of an apartment block which is shown in Figure 6 d). Location of the buildings is indicated in Figure 1. Bottom: Corresponding H/V spectral ratio of the soil. Please note the different amplitude scaling for the H/V spectral ratios.

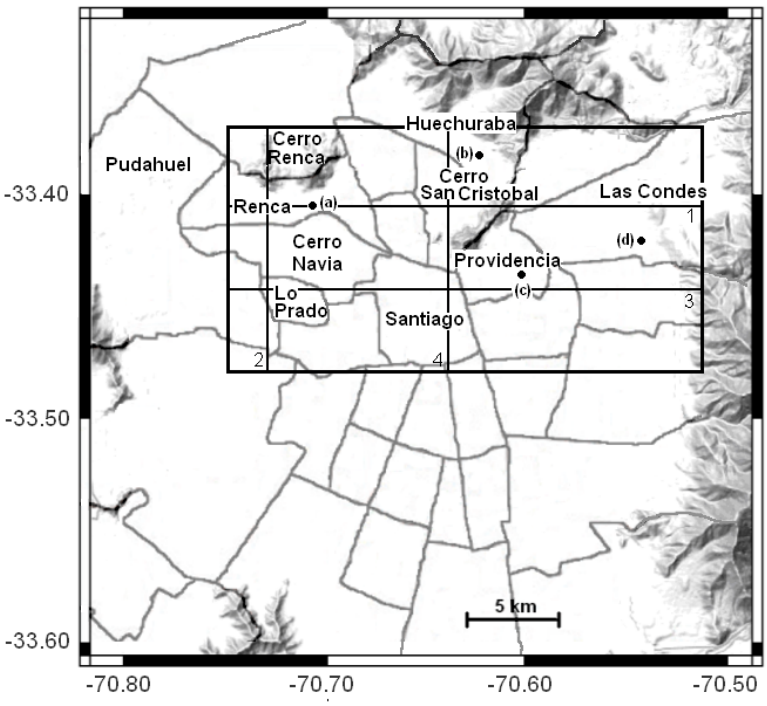
Huechuraba
Cerro
Renca
(b)
Pudahuel
Cerro
San Cristobal
Las Condes
Renca
(a)
1
(d)
Cerro
Navia
Providencia
(c)
3
Lo
Prado
Santiago
2
4
5 km
-33.40
-33.50
-33.60
-70.80
-70.70
-70.60
-70.50

Figure 1

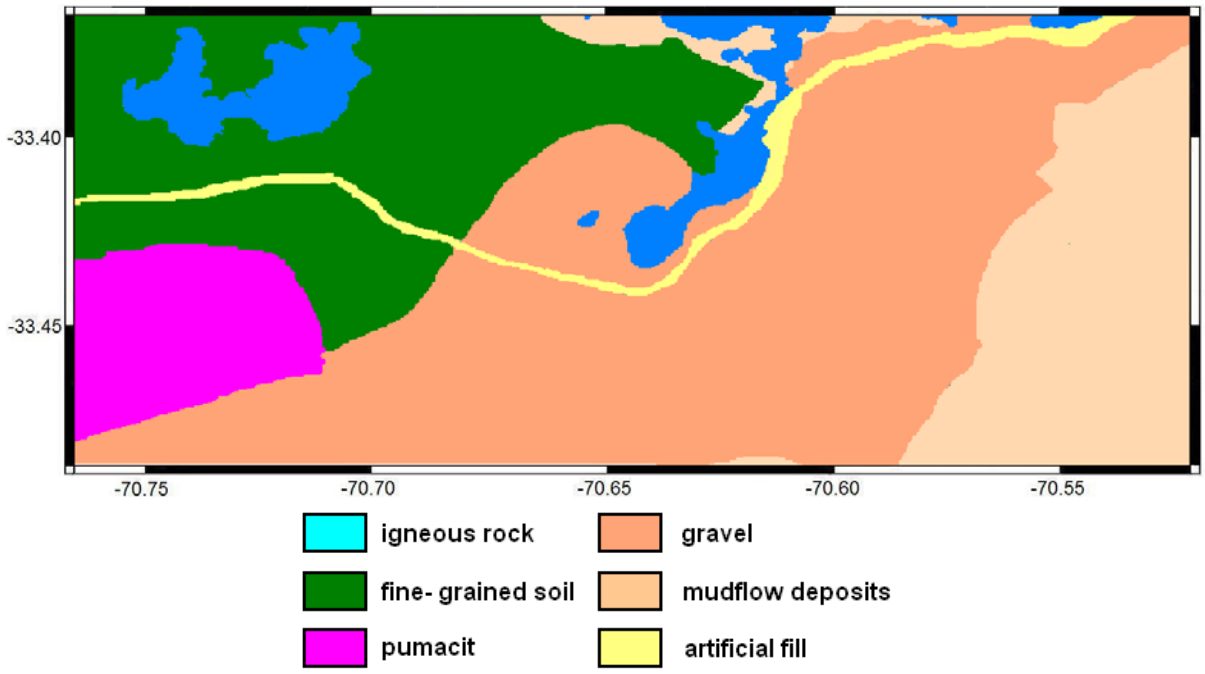
-33.40
-33.45
-70.75
-70.70
-70.65
-70.60
-70.55
igneous rock
gravel
fine- grained soil
mudflow deposits
pumacit
artificial fill

Figure 2

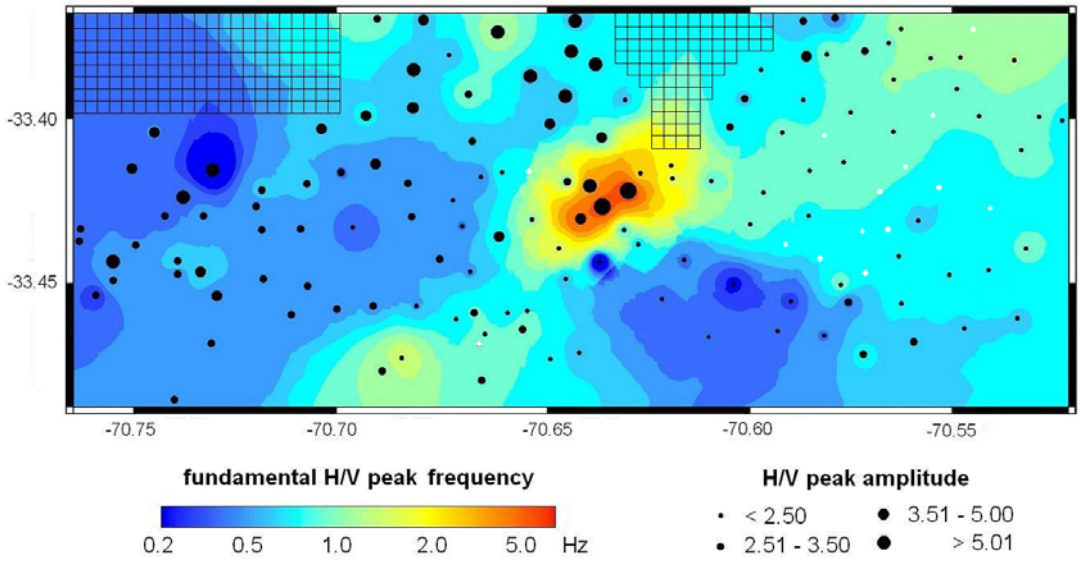
-33.40
-33.45
-70.75
-70.70
-70.65
-70.60
-70.55
fundamental H/V peak frequency
0.2
0.5
1.0
2.0
5.0
Hz
H/V peak amplitude
< 2.50
2.51 - 3.50
3.51 - 5.00
> 5.01

Figure 3

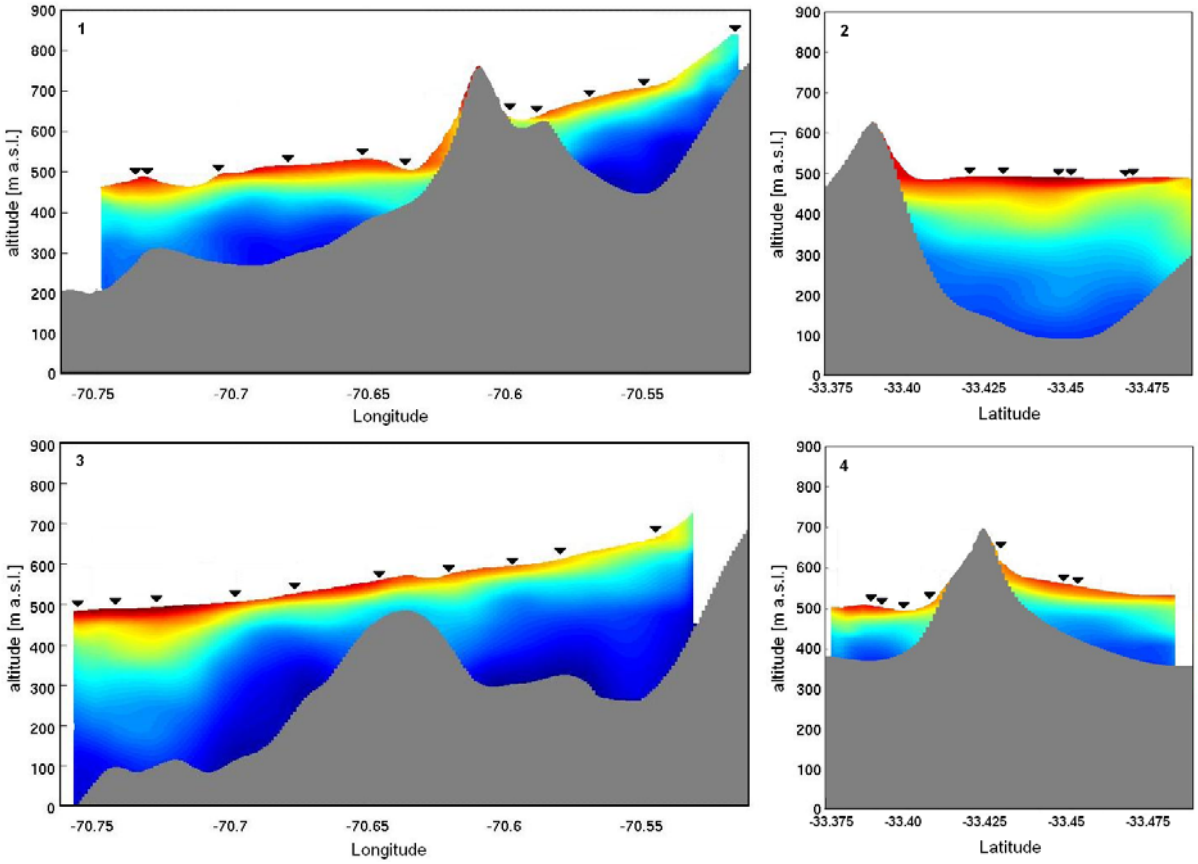
1
2
3
4
altitude [m a.s.l.]
Longitude
Latitude
900
800
700
600
500
400
300
200
100
0
-70.75
-70.7
-70.65
-70.6
-70.55
-33.375
-33.40
-33.425
-33.45
-33.475

Figure 4

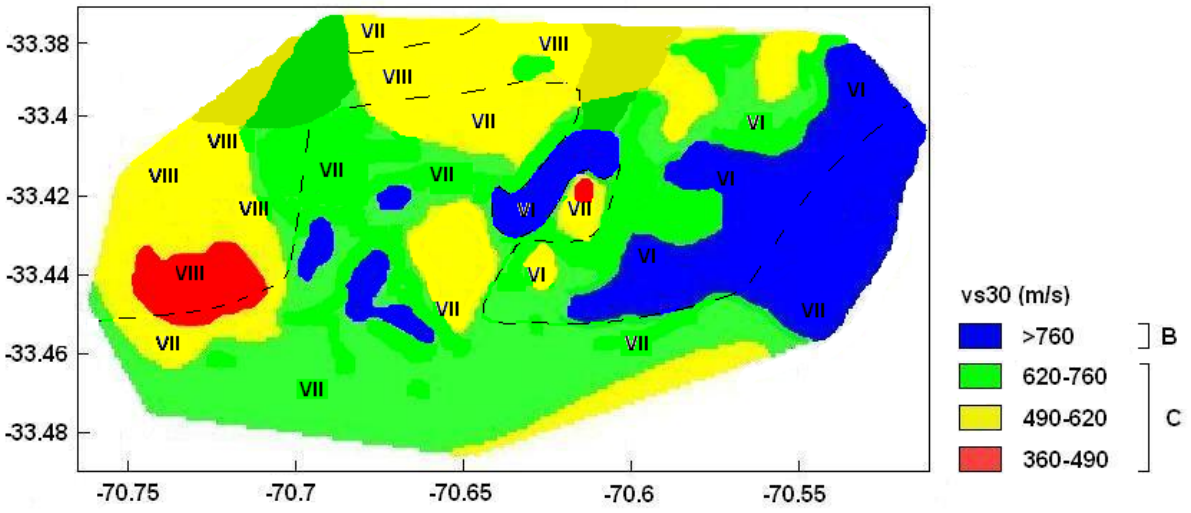
-33.38
-33.4
-33.42
-33.44
-33.46
-33.48
-70.75
-70.7
-70.65
-70.6
-70.55
VII
VIII
VI
vs30 (m/s)
>760
620-760
490-620
360-490
B
C

Figure 5

a)

b)

c)

d)

Figure 6

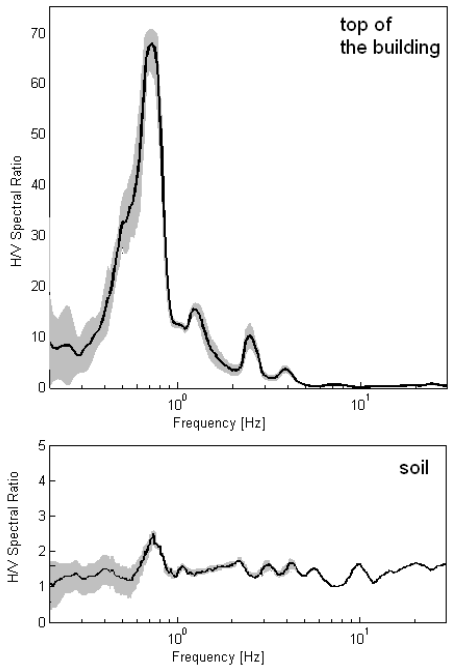
top of
the building
H/V Spectral Ratio
Frequency [Hz]
soil
H/V Spectral Ratio
Frequency [Hz]

Figure 7